Spectral-weight transfer: Breakdown of low-energy-scale sum rules in correlated systems

M. B. J. Meinders
Materials Science Centre, Department of Solid State and Applied Physics, University of Groningen, Nijenborgh 4, 9747 AG Groningen, The Netherlands

H. Eskes
Max-Planck-Institut für Festkörperforschung, Heisenbergstrasse 1, D-7000 Stuttgart 80, Federal Republic of Germany

G. A. Sawatzky
Materials Science Centre, Department of Solid State and Applied Physics, University of Groningen, Nijenborgh 4, 9747 AG Groningen, The Netherlands

(Received 4 March 1993)

In this paper we study the spectral-weight transfer from the high- to the low-energy scale by means of exact diagonalization of finite clusters for the Mott-Hubbard and charge-transfer model. We find that the spectral-weight transfer is very sensitive to the hybridization strength as well as to the amount of doping. This implies that the effective number of low-energy degrees of freedom is a function of the hybridization and therefore of the volume and temperature. In this sense it is not possible to define a Hamiltonian which describes the low-energy-scale physics unless one accepts an effective nonparticle conservation.

I. INTRODUCTION

In spite of a lot of theoretical and experimental studies, there is still little understanding about the normal-state excitation spectrum, and therefore of the low-energy-scale physics, of (strongly) correlated systems. Because the full many-body Schrödinger equation is not solvable, one is forced to make approximations to describe the (low-energy) physics of correlated materials. The first thing usually done is to construct a model Hamiltonian, which incorporates the most important characteristics of strongly correlated systems. However, even the one-dimensional Mott-Hubbard (MH) model, which is one of the least complicated realistic model Hamiltonians, is not fully understood. Although one has established that the low-energy physics of the one-dimensional MH model, which has been solved by Lieb and Wu,[1] can be described in terms of spinons and holons,[2] the extraction of the relevant physical information is still a problem.[3] The two- and three-dimensional MH model as well as the three-band charge-transfer (CT) model, where an uncorrelated band exists between the lower Hubbard band (LHB) and the upper Hubbard band (UHB) (as in the high T_c's) have not been solved yet, and the description of the low-energy physics is a very interesting field of proposals and intelligent guesses.

For understanding the low-energy physics, further approximations have to be made. Often one treats the on-site Coulomb repulsion in a mean field way as in a homogeneous or inhomogeneous[4] Hartree-Fock (HF) calculation with the addition of random-phase approximation to describe optical and spin excitations.[5] To reduce the Hilbert space and thereby hopefully the complexity of the problem, one projects out the high-energy states (doubly occupied states) completely, as one does when reducing the three-band Emery model[6] or one-band Hubbard model to a t-J model.[7] A different strategy is to use a slave operator technique to project out double occupation. This results in a mean-field starting point for the calculation but has the advantage that the usual many-body techniques can be used to include correlations.[8]

Another approach is to diagonalize the model Hamiltonian exactly or use Monte Carlo methods, but then one is restricted to small finite clusters resulting in large energy spacings between the levels. These energy spacings for a one-dimensional chain of 20 sites or a two-dimensional 4×4 cluster is of the order of 50 meV or 600 K. This is much too large to describe the low-energy physics in detail.

The main purpose of all these mentioned approximations is generally aimed at finding some suitable effective Hamiltonian, which can be used to describe the low-energy-scale properties of solids. However, this search may be futile if it turns out that the low- and high-energy scales cannot be decoupled, or that such a decoupling is only valid provided one is willing to leave the concepts of fermion or Bose statistics[9] or perhaps even the comforts of well established sum rules.

In this paper we study, using exact diagonalization, one remarkable feature, out of many, of the normal-state excitation spectra, namely, the doping and hybridization dependence of the spectral weight transfer from the high- to the low-energy scale. A nice experimental example of this phenomenon is the O $1s$ x-ray absorption study[10,11] of the $La_{2-x}Sr_xCuO_4$ system, where, upon hole doping in the O $2p$ band, spectral intensity of the upper-Hubbard band (high-energy scale) is transferred to the low-energy scale near the Fermi edge. Similar behavior has experimentally been found for several correlated systems.[12,13] In a previous paper[14] we described the general physical

origin of this redistribution of spectral intensities and its doping dependence, while Hybertsen *et al.*[15] gave a description of the O K edge in particular. This occurrence of spectral weight transfer, which we believe is a fingerprint for correlation effects, is now commonly accepted and has been observed in several numerical calculations[16,17] of correlated systems.

In this paper we will study the spectral weight transfer in greater detail and describe the important consequences for the description of the low-energy physics. Furthermore, different approaches such as the so-called Hubbard I solution,[18] the t-J model and mean-field theories will be discussed with respect to the spectral weight transfer.

In Sec. II we review the differences between doping a semiconductor, a localized MH and a CT system. In Sec. III the influence of the hybridization for the MH (Sec. III A) and CT system (Sec. III B) is taken into account. The results will be discussed and compared with other theories in Sec. IV, while also the consequences will be considered. Conclusions are given in Sec. IV.

II. COUNTING PRINCIPLE

An interesting question is what happens with the low-energy scale states if we dope a strongly correlated insulator as for example in $Li_xNi_{1-x}O$ or $La_{2-x}Sr_xCuO_4$. We may study this by looking at the one electron Green's function. Assuming that there are N electrons in the ground state, we define the one electron removal Green's function as

$$G_\sigma^-(\mathbf{k},\omega)=\sum_m \frac{A_\sigma^-(\mathbf{k},\omega_m)}{\omega-E_m^{N-1}+E_{\rm GS}^N+i\eta} \ . \tag{1}$$

Here the summation runs over all $N-1$ particle final states with wave functions ψ_m^{N-1} and eigenenergies E_m^{N-1}. The pole strength is defined as

$$A_\sigma^-(\mathbf{k},\omega_m)=|\langle \psi_m^{N-1}|c_{\mathbf{k}\sigma}|\psi_{\rm GS}^N\rangle|^2 \ ,$$

where $c_{\mathbf{k}\sigma}$ annihilates an electron with momentum $\mathbf{k}$ and spin σ from the N-particle ground state $\psi_{\rm GS}^N$. The angular integrated photoelectron spectrum $W^{\rm PES}$ is now given by

$$W^{\rm PES}(\omega)=\sum_{\mathbf{k}\sigma} W_{\mathbf{k}\sigma}^{\rm PES}(\omega)=\sum_{\mathbf{k}\sigma}\frac{1}{\pi}\lim_{\eta\downarrow 0}{\rm Im}G_\sigma^-(\mathbf{k},\omega) \ . \tag{2}$$

In the same way the one-electron addition Green's function is given by

$$G_\sigma^+(\mathbf{k},\omega)=\sum_m \frac{A_\sigma^+(\mathbf{k},\omega_m)}{\omega-E_m^{N+1}+E_{\rm GS}^N-i\eta} \ . \tag{3}$$

with pole strength

$$A_\sigma^+(\mathbf{k},\omega_m)=|\langle \psi_m^{N+1}|c_{\mathbf{k}\sigma}^\dagger|\psi_{\rm GS}^N\rangle|^2 \ ,$$

where $c_{\mathbf{k}\sigma}^\dagger$ creates an electron with momentum $\mathbf{k}$ and spin σ into the ground state. The inverse photoelectron spectrum $W^{\rm IPES}$ is then given by

$$W^{\rm IPES}(\omega)=\sum_{\mathbf{k}\sigma} W_{\mathbf{k}\sigma}^{\rm IPES}(\omega)=\sum_{\mathbf{k}\sigma}\frac{1}{\pi}\lim_{\eta\downarrow 0}{\rm Im}G_\sigma^+(\mathbf{k},\omega) \ . \tag{4}$$

We note that the pole strengths $A_\sigma^\pm(\mathbf{k},\omega_m)$ are just the overlap between the eigenstates $\psi_m^{N\pm1}$ and the state obtained by suddenly adding or removing an electron from the ground state; thus

$$\begin{aligned} c_{\mathbf{k}\sigma}^\dagger\psi_{\rm GS}^N&=\sum_m A_\sigma^+(\mathbf{k},\omega_m)\psi_m^{N+1} \ , \\ c_{\mathbf{k}\sigma}\psi_{\rm GS}^N&=\sum_m A_\sigma^-(\mathbf{k},\omega_m)\psi_m^{N-1} \ . \end{aligned} \tag{5}$$

For an insulator, doped with x holes, we define the low-energy spectral weight (LESW) for a certain spin and momentum as

$$\begin{aligned} \Lambda_{\mathbf{k}\sigma}(x)&=\int_0^{\omega_g} W_{\mathbf{k}\sigma}^{\rm IPES}(\omega)d\omega \\ &=\int_0^{\omega_g} A_\sigma^+(\mathbf{k},\omega_m)\delta(\omega-E_m^{N+1}+E_{\rm GS}^N)d\omega \ , \\ \Lambda(x)&=\sum_{\mathbf{k}\sigma}\lambda_{\mathbf{k}\sigma}(x) \ . \end{aligned} \tag{6}$$

The LESW for an electron-doped insulator is defined as

$$\begin{aligned} \Lambda_{\mathbf{k}\sigma}(x)&=\int_0^{\omega_g} W_{\mathbf{k}\sigma}^{\rm PES}(\omega)d\omega \\ &=\int_0^{\omega_g} A_\sigma^-(\mathbf{k},\omega_m)\delta(\omega-E_m^{N-1}+E_{\rm GS}^N)d\omega \ , \\ \Lambda(x)&=\sum_{\mathbf{k}\sigma}\Lambda_{\mathbf{k}\sigma}(x) \ . \end{aligned} \tag{7}$$

The upper limit of integration ω_g is chosen somewhere in the correlation gap, which divides the high-energy states from the low-energy states. The chemical potential is set equal to 0. Thus $\Lambda(x)$ may be seen as the effective number of degrees of freedom in the low-energy regime, responsible for the low-energy physics.

Let us consider a semiconductor (which can be described in an independent particle framework) with an occupied valence band and an unoccupied conduction band, separated by an energy gap $E_{\rm gap}$. In this case the poles $G_\sigma(\mathbf{k},\omega)$ are positioned at just the one-particle energies $\epsilon_{\mathbf{k}\sigma}$, as derived from some sort of band theory. The pole strength $A_\sigma^\pm(\mathbf{k},\epsilon_{\mathbf{k}\sigma})$ is 1 or 0, depending on the occupation of the one electron levels. For the undoped semiconductor the total electron removal and addition spectrum will look as sketched in Fig. 1. If the total number of sites equals $\mathcal{N}$ then there are $2\mathcal{N}$ occupied states and $2\mathcal{N}$ unoccupied states, separated $E_{\rm gap}$. Suppose we chemically dope the semiconductor, resulting in the addition of one hole, then the chemical potential will shift into the former occupied band, provided we can neglect the impurity potential of the dopant. The total electron removal spectral weight will be $2\mathcal{N}-1$ (just the number of electrons in the ground state) and the total electron addition spectral weight will be $2\mathcal{N}+1$ (total number of holes in the ground state). We may divide the electron addition spectrum into two parts, a high-energy-scale part (the conduction band) and a low-energy-scale part, which is the unoccupied part of the valence band (see Fig. 1). We immediately see now that

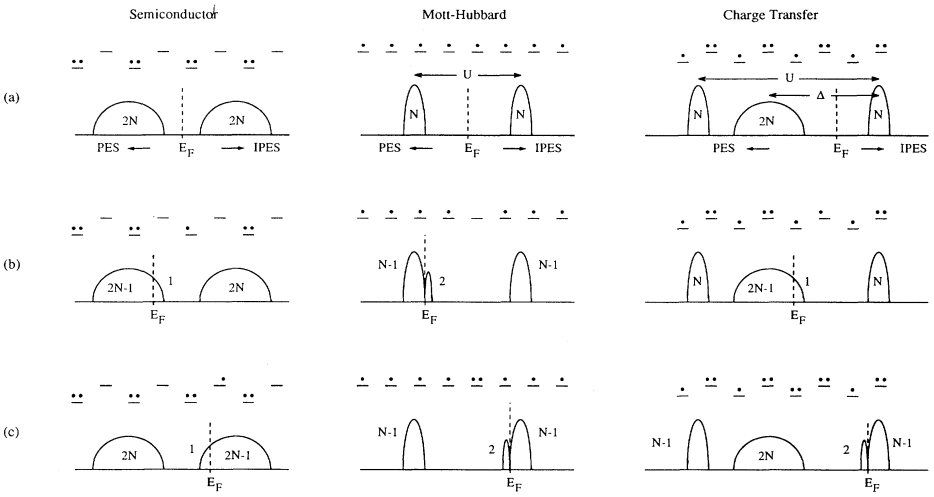

FIG. 1. A schematic drawing of the electron-removal and electron-addition spectra for a semiconductor (left), a Mott-Hubbard system in the localized limit (middle) and a charge transfer system in the localized limit (right). (a) Undoped (half filling), (b) one-electron doped, and (c) one-hole doped. The bars just above the figures represent the sites and the dots represent the electrons. The on-site repulsion U and the charge-transfer energy Δ are also indicated.

the LESW equals 1. The same arguments hold for an electron-doped semiconductor. Thus, when doping a semiconductor, the total spectrum is just given by a repositioning of the chemical potential and the LESW grows as x (with x the amount of doping). At the same time the spectral weight of the high-energy band is not changed. Thus, there is no redistribution of spectral intensities upon doping a simple semiconductor.

Consider now a correlated system described by the MH Hamiltonian. The one-band Hubbard Hamiltonian is defined as

$$H=t\sum_{\langle i,j\rangle,\sigma}(c_{i\sigma}^{\dagger}c_{j\sigma}+\text{H.c.})+U\sum_{i}c_{i\uparrow}^{\dagger}c_{i\uparrow}c_{i\downarrow}^{\dagger}c_{i\downarrow}\ , \tag{8}$$

where t is the hybridization between nearest-neighbor orbitals and U is the on-site repulsion. $\langle ij\rangle$ runs over all nearest-neighbor pairs, i runs over all sites. The $c_{i\sigma}^{\dagger}$ ($c_{i\sigma}$) creates (annihilates) an electron at site i with spin $\sigma=\uparrow,\downarrow$.

We first examine the one-particle Green's function for an $\mathcal{N}$-site MH cluster in the localized limit [$t=0$ in Eq. (8)] as a function of doping. In Fig. 1 (top middle) the total photoelectron and inverse photoelectron spectrum at half filling is shown. The total electron-removal spectral weight is equal to the number of occupied levels, while the total electron-addition spectral weight is equal to the number of unoccupied levels. Therefore, each has an intensity equal to $\mathcal{N}$. Upon doping the system with one hole, there are $\mathcal{N}-1$ singly occupied sites so the total electron removal spectral weight will be $\mathcal{N}-1$. For electron addition there are $\mathcal{N}-1$ ways for adding the electron to a site which was already occupied. Therefore the intensity of the UHB will also be $\mathcal{N}-1$ (not $\mathcal{N}$). We are left with the empty site for which there are two ways of adding an electron (spin up, spin down), both belonging to the LHB. Thus we find $\mathcal{N}-1$ electron removal states near the Fermi-level, two electron addition states near the Fermi level and $\mathcal{N}-1$ electron addition states in the UHB. The same arguments hold for the electron doped case. Thus (normalizing the total PES+IPES spectrum to 2), a doping concentration x yields a LESW $\Lambda(x)=2x$ and the high-energy spectral weight is $1-x$. There have been $\mathcal{N}x$ states transferred from high to low energy.

For the high-T_c superconductors, an oxygen band is located between the LHB and UHB. These systems therefore have to be described as a CT system.[19] A prototype charge-transfer Hamiltonian for CuO_2 planes in the cuprates reads

$$\begin{aligned}H=&\epsilon_d\sum_i d_{i\sigma}^{\dagger}d_{i\sigma}+\epsilon_p\sum_j p_{j\sigma}^{\dagger}p_{j\sigma}\\&+t_{pp}\sum_{\langle jj'\rangle,\sigma}(-1)^{\alpha_{jj'}}(p_{j\sigma}^{\dagger}p_{j'\sigma}+\text{H.c.})\\&+t_{pd}\sum_{\langle ij\rangle,\sigma}(-1)^{\alpha_{ij}}(p_{j\sigma}^{\dagger}d_{i\sigma}+\text{H.c.})\\&+U_{dd}\sum_i d_{i\uparrow}^{\dagger}d_{i\uparrow}d_{i\downarrow}^{\dagger}d_{i\downarrow}\ ,\end{aligned} \tag{9}$$

where i runs over all Cu sites and j over all O sites and $\langle ij\rangle$ represents a nearest-neighbor pair. $d_{i\sigma}^{\dagger}$ ($d_{i\sigma}$) creates (annihilates) a hole on a copper site, while $p_{i\sigma}^{\dagger}$ ($p_{i\sigma}$) creates (annihilates) a hole on an oxygen site. The charge-transfer energy Δ is defined as the difference between the on-site energy of O and Cu ($\Delta=\epsilon_p-\epsilon_d$). The hybridization between the nearest-neighbor oxygen orbitals has strength t_{pp} while the hybridization between a copper orbital and a nearest-neighbor oxygen orbital is t_{pd}. U_{dd} is the on-site Coulomb interactions between two holes on a copper site. The signs of t_{pd} and t_{pp} are described by α_{ij} and $\alpha_{jj'}$ which are 0 or 1, depending on the relative position of a nearest-neighbor copper-oxygen and oxygen-oxygen pair, respectively.

Assume first that we are dealing with a CT system in the localized limit, i.e., we do not allow any hybridization between the oxygen and copper sites ($t_{pd}=0$). Assume no holes in the oxygen band (as in the insulating compounds), then the one particle Green's function will look like that sketched in Fig. 1 (top right). When we dope this system with electrons, the situation is similar to the MH case and we find a spectral weight transfer from high to low energy. Thus in this case the LESW $\Lambda(x)=2x$. However, upon hole doping, the situation is similar to that of the semiconductor without any spectral weight

transfer. So, for the CT system in the localized limit, we find a fundamental asymmetry between hole and electron doping.

In the examples above we could find the LESW just by counting the available states, which can be reached when we do a photoelectron experiment or an inverse photoelectron experiment. This is because the oscillator strength $A_\sigma^{\pm}(\mathbf{k},\omega_m)$ is always one or zero, depending on whether the state is occupied or empty. This is always the case in theories where the Coulomb repulsion is treated in a mean-field way and where the photoelectron spectrum is equal to the density of states (DOS), i.e., when "spectral weight" can be replaced by "states." In local-density approximation (LDA) or restricted Hartree-Fock (HF) calculations the added holes will occupy $\mathbf{k}$ states, and the change in potential due to these holes will be evenly distributed over all sites and can therefore be neglected when $x \ll 1$. Therefore, we will always find a LESW $\Lambda(x)=x$. Inhomogeneous Hartree-Fock calculations[4,5] reveal that, for large U/t, upon doping a state can be pushed out from the upper Hubbard band to the Fermi level. In this case the LESW goes as $\Lambda=2x$, which looks like the ionic MH model. In this case the extra hole will form a local potential and therefore the counting principle for the ionic Hubbard model applies. Lowering U one can expect that this hole will spread out. This means that the extra state moves back to the upper Hubbard band or lies somewhere in the gap. This may be interpreted as $\Lambda(x)$ somewhere between x and $2x$. We shall show that this is not the expected behavior for a correlated system. Note that the definition of $\Lambda(x)$ becomes meaningless when the gap fills up.

Close to half filling and for $U \gg t$ the Hubbard model transforms into the t-J model. This model describes the antiferromagnetic interaction between two spins on neighboring sites and it allows for a restricted hopping between neighboring sites. The restriction consists of the fact that no doubly occupied sites are allowed. It means that we are only dealing with empty and singly occupied states and therefore again one can apply the above reasoning. Thus the LESW goes as $\Lambda(x)=2x$. While the factor $2x$ for the MH and CT model is really only valid in the ionic limit (t or $t_{pd}=0$), in the t-J model it is independent of the actual value of t and/or J. Thus the t-J model behaves as a single-band Hubbard model with $t=0$ for all values of the hybridization.

All these examples show a linear LESW with respect to the doping concentration. We also found that for the hole-doped CT model the LESW behaves like a simple semiconductor, i.e., $\Lambda(x)=x$. This is contrary to what is found experimentally for the high T_c's.[10,11] In the next section we will show that the hybridization yields a strong deviation from linear behavior of the LESW for the correlated MH and CT models and explains the experimental results.

III. INFLUENCE OF HYBRIDIZATION: DYNAMICAL SPECTRAL WEIGHT TRANSFER

We use exact diagonalization on small clusters to calculate the one electron Green's function $G_\sigma^-(\mathbf{k},\omega)$ for the MH and CT model. The Lanczos method as described in, for instance, Refs. 20 or 21 is used. We perform calculations for one- and two-dimensional MH clusters for different values of U/t as well as the CT model for different parameter values and we adopt periodic boundary conditions.

A. Mott-Hubbard model

All the calculations for the MH model [Eq. (8)] are performed with an on-site Coulomb repulsion $U=10$ eV. In Fig. 2 the total electron removal and addition spectra are plotted for a 10-site one-dimensional ring with $t=-1.0$ eV and for different number of electrons N. The hole (electron) doping concentration is given by $x=|(N-\mathcal{N})/\mathcal{N}|$ with the number of sites $\mathcal{N}=10$ ($N<\mathcal{N}$ corresponds to hole doping and $N>\mathcal{N}$ corresponds to electron doping). From the figure we see immediately that if we go from the one-hole- to one-electron-doped case, the chemical potential shifts by just the amount of the insulating gap. Therefore, there is no sign at all of a chemical potential which remains roughly halfway between the two bands due to doping-induced midgap

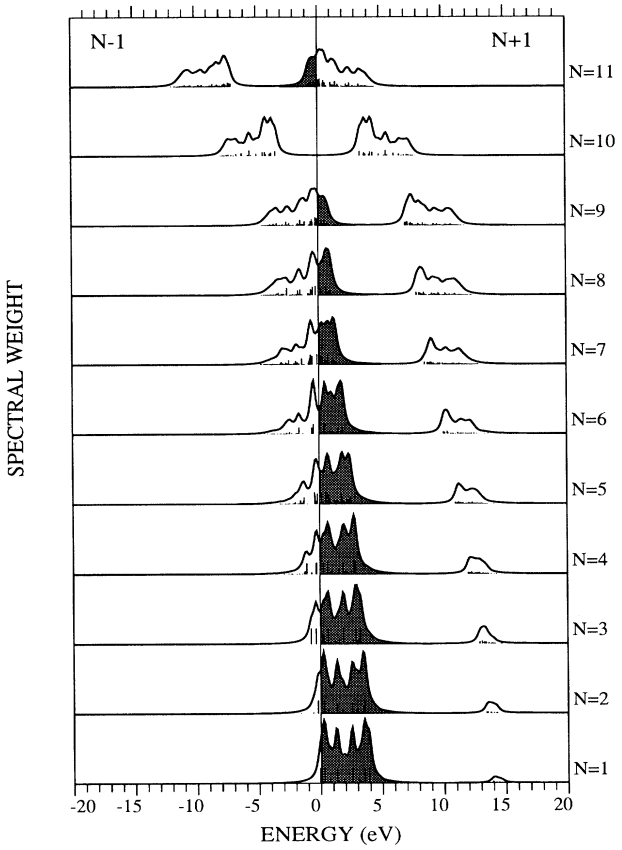

FIG. 2. One-particle Green's function for a one-dimensional Hubbard-ring of $N=10$ sites for $U=10$ eV and $t=1$ eV. The number of electrons in the ground state N are indicated. The low-energy electron-addition spectral weight is obtained by integration over the shaded area.

states,[22] in agreement with Ref. 23 but in contrast to the suggestion by Allen *et al.*[24] We observe the same kind of chemical potential shift for other values of t.

The LESW, as defined by Eq. (6), is obtained by integrating the shaded area. In Fig. 3 we plotted the low-energy electron addition spectral weight for the 10-site cluster from $t=-0.5$ to -2.0 eV in steps of 0.25 eV. For strong hybridization it is no longer possible to define ω_g properly for all doping concentrations because, due to hybridization, incoherent parts of $G(\mathbf{k},\omega)$ are spread through the gap. There is therefore no clean distinction between the low- and high-energy scale. However, for large doping concentrations and large hybridization it may still be possible to define ω_g because of an increase of the gap with doping. This phenomenon is clearly seen in Fig. 2. The observed increase of the original insulating gap with increasing doping concentration is contrary to what is usually found in mean-field-like theories, where the effective on-site repulsion is proportional to the expectation value of the electron density, $U_{\text{eff}}=U\langle n_i\rangle$. Therefore, the gap always has the tendency to collapse with doping because of a decrease of the effective interaction. The increase of the gap in the exact diagonalization with doping has a simple physical origin. Increasing the hole-doping concentration results in an increase of the number of $N+1$-particle states at the Fermi edge with which the states in the UHB can hybridize. This will push these two bands apart and cause an increase of the gap between the low- and high-energy scale states.

It is also interesting to note that mean-field theory gives correct first moment, i.e., the energy average. The first moment for the combined photo-emission and inverse-photo-emission spectrum is given by

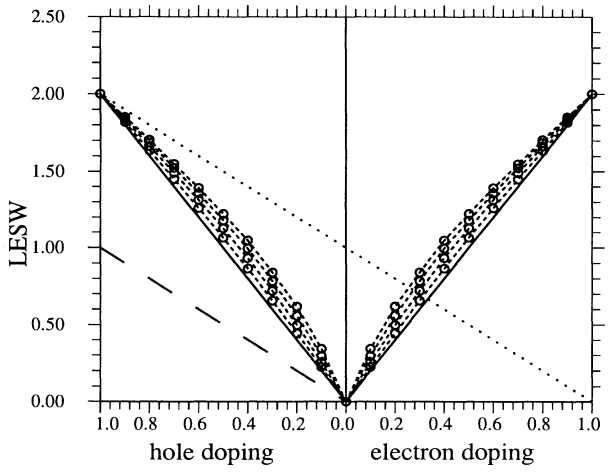

FIG. 3. The integrated LESW divided by the number of sites as a function of the doping concentration x for the one-dimensional ten-site Hubbard ring ($U=10$ eV). The solid lines correspond to the localized limit $t=0$, the dotted line to the free particle limit (hole doped) and the dashed line to hole doping a semiconductor. The data points are from the calculations: $t=-0.5$ eV (lowest) to $t=-2$ eV steps of 0.5 eV.

$$m_1=\frac{1}{\mathcal{N}}\sum_{i,\sigma}\langle\{[c_{i\sigma}^{\dagger},H],c_{i\sigma}\}_+\rangle \tag{10}$$

where $\langle\ \rangle$ is the expectation value in the exact ground state. Substituting the MH Hamiltonian [Eq. (8)] we find for the first moment $m_1=Un=U(N/\mathcal{N})$, where n is the number of electrons per site. For paramagnetic Hartree-Fock we have

$$H_{\text{HF}}=\sum_{\mathbf{k},\sigma}(\epsilon_{\mathbf{k}}+U\langle n_{i\sigma}\rangle)c_{\mathbf{k}\sigma}^{\dagger}c_{\mathbf{k}\sigma}\ . \tag{11}$$

Since the average of the band energies $\epsilon_{\mathbf{k}}$ equals 0, the HF and exact first moments are identical for a homogeneous charge distribution. The same holds for antiferromagnetic HF. However, in HF this correct first moment is generally obtained by changing the eigenenergies with doping, while the weights remain unchanged (equal to 1). This is contrary to exact diagonalization, where the eigenenergies change only little and the correct first moment is obtained by modifying the weights.

In Fig. 3 we also show $\Lambda(x)=x$ corresponding to hole doping a semiconductor as well as the free-particle limit. In the free particle limit there is no high-energy scale so the LESW goes as $\Lambda(x)=x+1$, i.e., $\Lambda(x)=1$ for zero doping (half-filled band) and $\Lambda(x)=2$ for an empty or full band.

From the figure we see that the low-energy spectral weight grows even faster than twice the amount of doping and that it is increasing with increasing $|t|$. At first glance this result is surprising because on increasing $|t|$ we would expect the LESW to go towards the one-particle theory result, which is $\partial\Lambda(x)/\partial x=1$, but instead we go even further away from it. Note that the slope for large doping, close to the empty or full band situation, goes towards the independent particle limit.

The-lowing doping regime for finite t can be understood as follows. We may write the final-state and ground-state wave function as a sum of states belonging to the UHB and of states belonging to the LHB. When calculating the oscillator strength

$$A_{\sigma}^{+}(\mathbf{k},\omega_m)=|\langle\psi_m^{N+1}|c_{\mathbf{k}\sigma}^{\dagger}|\psi_{\text{GS}}^{N}\rangle|^2$$

the phases of the wave functions will constructively interfere for transitions to the low-energy regime and destructively interfere for transitions to the high-energy regime, thereby increasing the LESW. This is a situation similar to one encountered in both core-level and valence-band spectral weights of CE, Kondo-like systems, in which the lowest-energy state obtains more weight than expected from the occupation numbers.[25] $\Lambda(x)>2x$ appears strange because it looks like there is room for much more than one electron per spin and per $\mathbf{k}$ state in the low-energy scale whereas we know that the total number of electrons we can add in the low-energy regime to reach again the insulator cannot be more than the hole-doping level. However, in a many-body system the phase space available to add one electron is larger than the number of electrons you can add in the low-energy scale.

If we substract the static part [the $\Lambda(x)=2x$ part, which comes from the counting of available states] we are left with the dynamical part of the LESW [DLESW: $\Lambda_D(x)=\Lambda(x)-2x$], due to the kinetic energy of the elec-

trons. In Fig. 4 the DLESW for the MH system is shown as well as $\Lambda_D(x)=1-x$, corresponding with the free-particle limit and $\Lambda_D(x)=-x$, corresponding with the semiconductor.

Also shown are the results of Harris and Lange[26] for two values of t (-0.5 and -2.0 eV). They worked out a first-order expression in t/U for the spectral weights in the lower and upper Hubbard bands. For the total integrated (i.e., PES and IPES) spectral weight of the LHB (which is the zeroth-order moment $m^0_{\rm LHB}$) they found

$$m^0_{\rm LHB}=\sum_\sigma \left[1-\langle c^\dagger_{i\bar\sigma}c_{i\bar\sigma}\rangle-\frac{2t}{N}\sum_{\langle ij\rangle}\langle c^\dagger_{i\bar\sigma}c_{j\bar\sigma}\rangle\right], \quad (12)$$

where $\langle ij\rangle$ runs over all nearest-neighbor pairs. Making use of the sum rules and assuming a homogeneous charge distribution, it is now a straightforward exercise to derive from Eq. (12) the LESW:

$$\Lambda(x)=2x-\frac{2t}{N}\sum_{\langle ij\rangle,\sigma}\langle c^\dagger_{i\bar\sigma}c_{j\bar\sigma}\rangle . \quad (13)$$

The first term describes the LESW for the MH model in the localized limit [$\Lambda(x)=2x$]. The second term is always positive and proportional to the expectation value of the kinetic energy. To calculate this expectation value, one has to use the zeroth-order ($U\to\infty$) wave functions, which are equivalent to the spinless-fermion wave function. They are given by filling up the one-particle momentum levels [$\epsilon_k=2t\cos(ka)$] with only one electron per state up to the Fermi wave vector. Doing so, we find a simple expression for the first order in t/U contribution to the DLESW:

$$\Lambda_D(x)=\frac{4|t|}{\pi U}\sin(\pi x) . \quad (14)$$

From the figure we see that this first-order term (proportional to the kinetic energy) gives a good approximation to the DLESW for small t as expected. However, the Harris-Lange result is symmetric around $x=0.5$. This is quite different from the exact diagonalizations for larger $|t|$ values where we find that this dynamical part is highly asymmetric and that the maximum of the DLESW lies somewhere in the doping range $x<0.4$. For small doping concentration the DLESW obtained from the exact calculations is substantially larger than that from the first-order approximation.

An often used approximation for the MH model is the Hubbard I decoupling scheme, proposed by Hubbard.[18] This approximation yields two poles for every momentum and spin with energies and pole strengths dependent on the occupation number in the ground state. The energies $E^{(1)}_{k\sigma}$ and $E^{(2)}_{k\sigma}$ ($E^{(1)}_{k\sigma}<E^{(2)}_{k\sigma}$) are given by

$$E^{(1),(2)}_{k\sigma}=\tfrac{1}{2}(U+\epsilon_k)\pm\tfrac{1}{2}\sqrt{(U-\epsilon_k)+4n_{-\sigma}U\epsilon_k} , \quad (15)$$

where ϵ_k are the one-particle energies (the center of the band is chosen to be 0). The pole strength for each pole can be found by differentiating the pole energies with respect to ϵ_k; thus,

$$A^{(1),(2)}_{k\sigma}=\frac{\partial E^{(1),(2)}_{k\sigma}}{\partial\epsilon_k} . \quad (16)$$

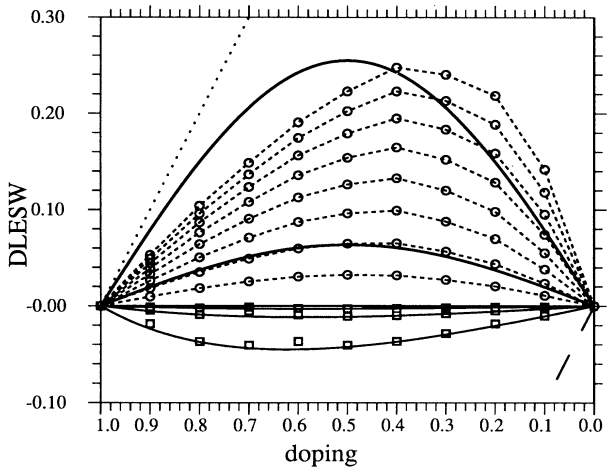

FIG. 4. The dynamical part of the LESW [$\Lambda_D(x)=\Lambda(x)-2x$] as a function of (hole) doping concentration x_h for the MH model. The dotted line corresponds to the free-particle limit (hole doped) and the dashed line to the semiconductor. The data points (○) are from the calculations: $U=10$, $t=-0.25$ eV (lowest) to $U=10$, $t=-2$ eV (highest) in steps of 0.25 eV. The first order in t/U results are shown in the upper part of the figure for $U=10$, $t=-0.5$ (lower solid curve) and $t=-2.0$ eV (upper solid curve). Also shown are results of the Hubbard I approximation in the lower part of the figure. The data points (□) correspond to the Hubbard I decoupling using ground state occupation numbers.

If we put the occupation number in the ground state for the up spins equal to the occupation number for the down spins it is straightforward to calculate the DLESW by filling the momentum energy levels up to the chemical potential, weighted by the pole strengths. The results are the solid lines ($t=0.5$, 1, and 2 eV) plotted in Fig. 4. The open squares are obtained by substituting the occupation numbers for the up and down spins as obtained from the exact diagonalized ground state of the 10-site cluster. From Fig. 4 it can be seen that the dynamical contribution to the LESW is negative, contrary to what is found in the exact diagonalization. As far as the LESW is concerned, the Hubbard I approximation has the tendency to go to the situation of doping a semiconductor, while the exact diagonalization has the tendency to go to the right free-particle limit for large hole or electron doping away from half filling.

In Figs. 5 and 6 we plot the derivative of the LESW with respect to the doping concentration x and the hybridization strength t, respectively. We again see that the LESW is a strong function of the hybridization t and doping concentration x. This means that the effective number of degrees of freedom in the low-energy regime (responsible for the low-energy physics) is strongly dependent on the hybridization and therefore on the volume and temperature of the system.

It is interesting to see what will happen with the electrons if the volume of a system is changed. Suppose we contract one half of a material, which results in an in-

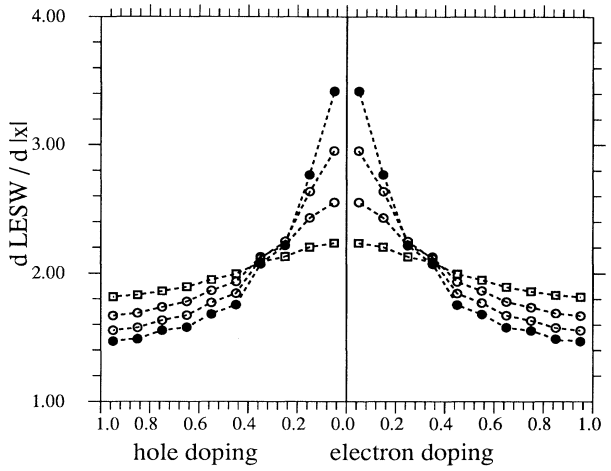

FIG. 5. The derivative of the LESW (see Fig. 3) with respect to the doping concentration for the MH model ($U=10$ eV): $t=-0.5$ (□) to $t=-2$ (●) in the steps of 0.5 eV.

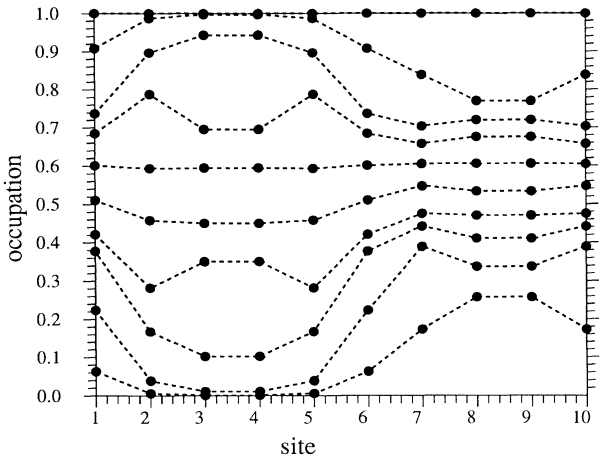

FIG. 7. The number of electrons per site for a one-dimensional MH chain ($U=10$ eV) for different values of the (hole-) doping concentration x_h. The lowest corresponds to $x=0.9$ and the highest to the undoped case ($n=1$, for all sites). The hybridization strength in the left part of the chain is 0.5 eV, while in the right part of the chain it is 1.0 eV.

crease of the hybridization in this region. If this material can be described by an independent particle picture, the electrons will go to that part of the sample with the largest hybridization as long as the band is less than half filled. Thus, if we are dealing with a hole-doped system, the number of electrons in the part with the largest volume will be lower than that in the part with smaller volume. However, if we are dealing with a correlated system the situation is really different. This is illustrated in Fig. 7. We consider a 10-site MH cluster. The Coulomb repulsion on every site is again 10 eV and the hybridization in the "left" part (sites 1–5) is 0.5 eV, while the hybridization in the right part of the cluster (sites 6–10) is 1.0 eV. We plotted the number of electrons per site for different values of the doping concentration. The lowest curve corresponds to a doping concentration $x=0.9$ and the upper curve to half filling.

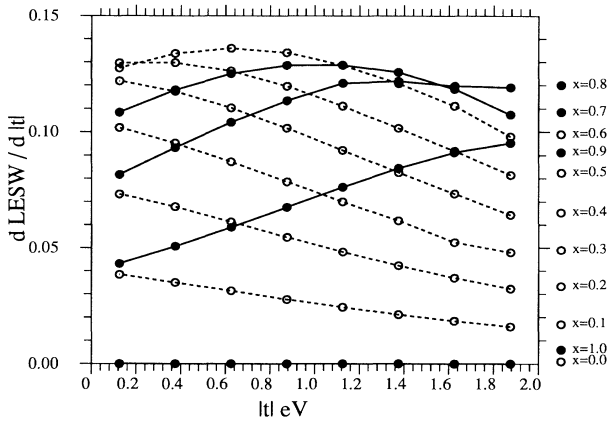

FIG. 6. The derivative of the LESW (see Fig. 3) with respect to the hybridization for the MH model ($U=10$ eV). The doping concentrations are indicated.

From the figure it can be seen that for small electron concentrations (large doping concentrations) the situation resembles more or less the independent particle limit where the electrons tend to go to the part with the largest hybridization. However, this picture changes when we approach a critical doping concentration of roughly 0.4. At this point the electrons are distributed homogeneously. When we decrease the doping concentration still further the role of electrons and holes are interchanged. For low hole doping concentration, the holes tend to go to the region with largest hybridization and not the electrons.

This may be compared with the electron-hole distribution in the $U\rightarrow\infty$ ground state. This is the spinless fermion ground state and is constructed by filling up the one-particle moment levels with only one electron. The one-dimensional band structure for spinless fermions for this system consists of two bands, one with high dispersion (corresponding with the right side of the sample) and one with lower dispersion (corresponding with the left side). Upon filling the system, we start filling up the band with highest dispersion until the one-particle energy level reaches the bottom of the other hand. Until this point is reached, all electrons go to the right side of the sample, where they gain most kinetic energy. From here, we fill up both bands. At exactly quarter filled, the number of electrons at both sides are equal, after which the role of electrons and holes are interchanged. This turning point can be seen to coincide with the critical doping concentration for which a maximum in the DLESW is obtained. This critical point moves towards lower doping concentrations when t/U is increased.

We also studied the effect of the cluster size as well as the dimensionality of the system on the LESW. We performed calculations on one-dimensional six-, eight-, and ten-site as well as for two-dimensional nine- and ten-site MH clusters. In order to be able to compare the one-

dimensional and two-dimensional systems, we adjust the hybridization in such a way that the same effective bandwidth is obtained. We define the one particle effective bandwidth as the root mean square value of the one particle energies, which equals the second moment $(zt^2$, with z the number of nearest neighbors, thus $t_{1D}=\sqrt{2}t_{2D}$). The DLESW for the one- ($t=-1$ eV) and two-dimensional ($t=-\sqrt{1/2}$ eV) clusters are shown in Fig. 8. For the one-dimensional systems, no substantial differences in the DLESW can be seen, from which we may conclude that the cluster size is of no qualitative importance as far as the DLESW is concerned. Also the two-dimensional clusters compare very well with the one-dimensional clusters provided the one-particle effective bandwidth is kept constant. From this comparison we may conclude that the phenomenon of spectral weight transfer is qualitatively and quantitatively independent of cluster size and dimensionality.

B. Charge-transfer model

It can be shown that the periodic two-dimensional Cu_4O_8 cluster, studied before as representing the CuO_2 planes of the cuprates,[20,27–29] is equivalent to the periodic one-dimensional Cu_4O_4 cluster if the onsite O-O repulsion is neglected (as we do). Because in the Cu_4O_8 cluster there are four pairs of equivalent oxygens, one can take linear combinations of these pairs. One linear combination does not couple to the Cu sites and forms nonbonding levels. Therefore, the two-dimensional Cu_4O_8 cluster reduces to a one-dimensional Cu_4O_4 chain with $\alpha_{jj'}=a_{ij}=0$ in Eq. (9), and $t_{pd,1D}=\sqrt{2}t_{pd,2D}$ and $t_{pp,1D}=-2t_{pp,2D}$. We perform calculations on the one-dimensional four-unit-cell (eight site) CT model (Cu_4O_4) with a copper on-site repulsion $U_{dd}=8$ eV, charge-transfer energy $\Delta=\epsilon_p-\epsilon_d=4$ eV, and oxygen-oxygen hybridization $t_{pp}=-0.25$ eV. The above relations for the hybridizations can be used to translate our results to the two-dimensional Cu_4O_8 cluster.

The total electron removal and addition spectra for the CT system with $t_{pd}=1$ eV and for different hole fillings are plotted in Fig. 9. The oxygen spectral weight is represented by the dotted line and the copper spectral weight by the solid line. The number of holes N in the ground state is indicated. The insulating CT system corresponds to the spectrum with four holes in the ground state. Thus the hole doping concentration is given by $x_h=(N-\mathcal{N})/\mathcal{N}(N\geq\mathcal{N})$ with $\mathcal{N}=4$ the number of unit cells. The electron doping concentration is given by $x_e=(\mathcal{N}-N)/\mathcal{N}(N\leq\mathcal{N})$. As in the MH case we find that the chemical potential shifts by just the amount of the insulating gap when we go from the one hole to the one-electron-doped system.

The LESW, obtained by integrating the d and p spectral weights over the shaded area, is shown in Fig. 10 for different values of t_{pd}. Again, we only focus on those values of t_{pd}, which ensures a sensible definition of ω_g. From the figure it can seen that the LESW as a function of the hybridization for electron-doped CT system

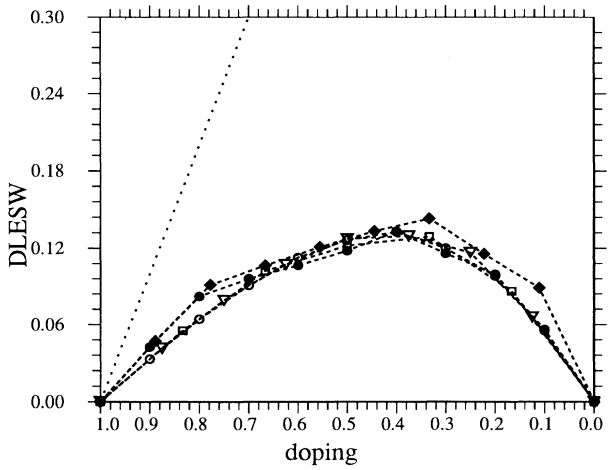

FIG. 8. The dynamical part of the LESW $[\Lambda_D(x)=\Lambda(x)-2x]$ as a function of (hole-) doping concentration x_h for the MH model for the one-dimensional ten-site (○), eight-sites (▽), and six-site (□) clusters with $U=10$ and $t=-1$ eV and two-dimensional ten-site (●) and nine-site (■) clusters with $U=10$ and $t=-0.71$ eV.

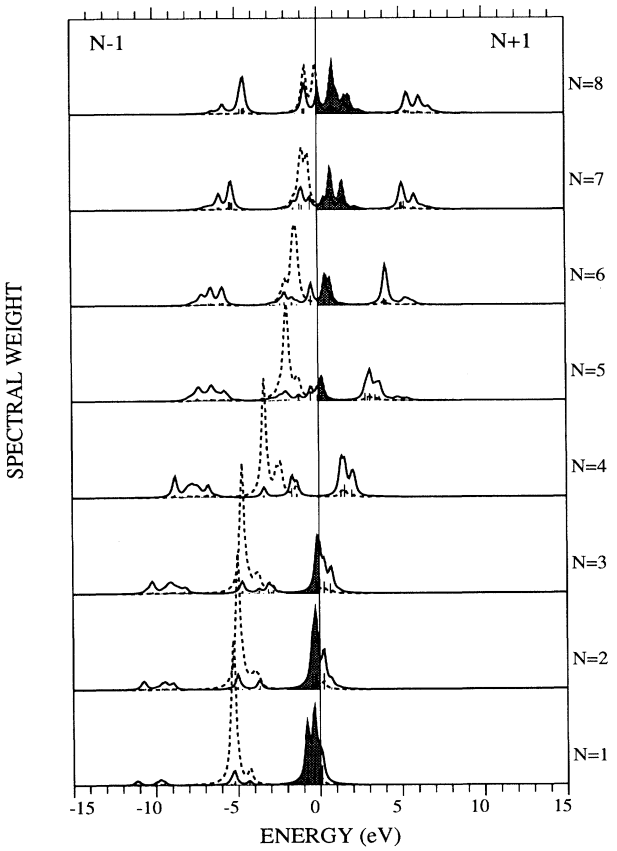

FIG. 9. One-particle Green's function for a one-dimensional four-unit-cell CT model. The dotted lines correspond to the p spectral weight and the solid lines to the d spectral weight. $U_{dd}=8$ eV, $t_{pd}=1$, $t_{pp}=-0.25$, and $\Delta=4$ eV. The number of holes in the ground state N are indicated. The LESW is obtained by integration over the shaded area.

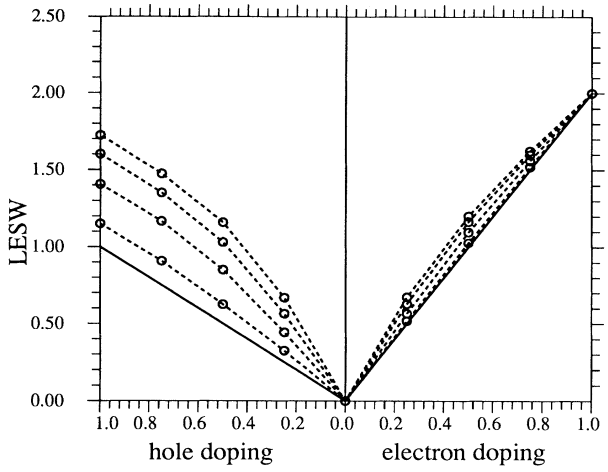

FIG. 10. The integrated total-LESW divided by the number of sites as a function of the doping concentration x for the one-dimensional four-unit-cell CT system ($U_{dd}=8$ eV), $t_{pp}=0.25$, $\Delta=4$ eV). The solid lines correspond to the localized limit $t_{pd}=0$. The data points are from the calculations: $t_{pd}=0.5$ eV (lowest) to $t_{pd}=2$ eV in steps of 0.5 eV.

behaves more or less the same as found for the MH system. However, for the hole-doped case, the situation is quite different. For small hybridization between the free-particle-like oxygen orbitals and correlated copper orbitals it is found that the LESW behaves semiconductorlike and every added hole adds a weight 1 to the total spectrum. But when the hybridization is increased, the LESW for the hole-doped CT system rapidly increases and the LESW becomes almost symmetric with respect to hole or electron doping for $t_{pd}=-2$ eV. This can also be seen from the derivative of the LESW with respect to the doping concentration as plotted in Fig. 11, which also shows a more or less symmetric figure with respect to hole and electron doping for large hybridization. It is interesting to note that the high-T_c superconductors lie in the regime with large hybridization, so the holes in the hole-doped high T_c's will behave as strongly correlated particles.

Due to the hybridization between the correlated Cu and free-electron-like O orbitals a sort of mirror LHB appears at the low-energy side of the oxygen band and the d spectral weight is strongly enhanced. This can also be seen in Fig. 9. Holes in this sort of Zhang-Rice singlet band[30] will behave as strongly correlated particles with restriction on double occupancy. This is also shown by Feiner,[31] who projected the CT model onto CuO_4 cell-eigenstates. This permits a description of the low-energy physics by an effective MH model with an effective U in the order of Δ. The set of cell eigenstates is a reduced set of eigenstates of a CuO_4 cluster, namely the zero-hole vacuum state, one-hole state (linear combination of p and d) and the two-hole Zhang-Rice singlet. The LESW can now be described as a sum of intracellular [result of the relation between the physical particles (holes) and the effective particles (cell-eigenstates)] and intercellular contributions (result of an effective MH model working on the effective particles). The intracell contribution is linear with doping. For electron doping it goes as $2x_e$, while for hole doping the intracell LESW equals cx_h with c between 1 ($t_{pd}=0$) and 2 ($t_{pd}\rightarrow\infty$). It turned out that the prefactor c, which reflects the internal hybridized nature of the cell states and can be calculated from the model parameters, is equal to the LESW at $x_h=1$, as found in the exact diagonalizations. The further increase of the LESW results from the intercell contributions and is shown in Fig. 12. This part may be seen as the kinetic

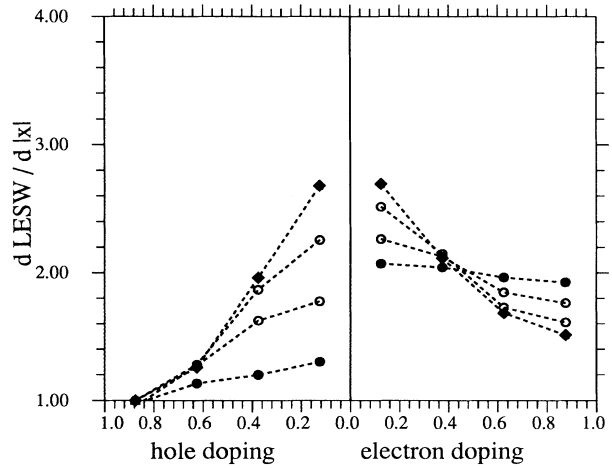

FIG. 11. The derivative of the LESW (see Fig. 10) with respect to the doping concentration for the CT model ($U_{dd}=8$, $t_{pp}=-0.25$, $\Delta=4$): $t_{pd}=0.5$ (□) to $t_{pd}=2$ eV (●) in steps of 0.5 eV.

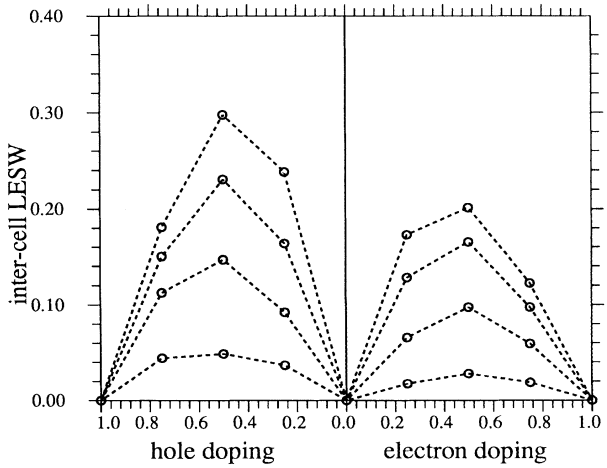

FIG. 12. The intercell contributions (see Ref. 31) to the LESW (see Fig. 10) with respect to the doping concentration for the CT model ($U_{dd}=8$, $t_{pp}=0.25$, $\Delta=4$). The intercell contribution equals LESW$-2x_e$ for electron doping and LESW$-cx_h$ for hole doping with c describing the internal hybridized nature of the CuO_4 cell eigenstates. The data points are from the calculations: $t_{pd}=0.5$ eV (lowest) to $t_{pd}=2$ eV in steps of 0.5 eV.

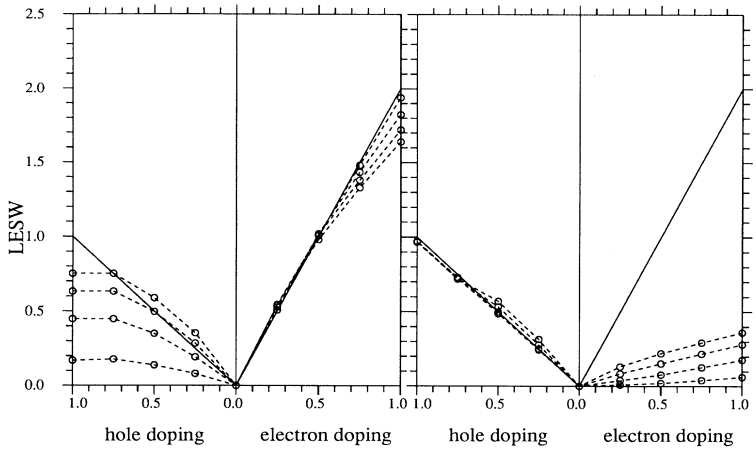

FIG. 13. The integrated d-LESW (left) and p-LESW (right) divided by the number of sites as a function of the doping concentration x for the one-dimensional four-unit-cell CT system ($U_{dd}=8$ eV, $t_{pp}=0.25$, $\Delta=4$ eV). The solid lines correspond to the localized limit $t_{pd}=0$. The data points are from the calculations: $t_{pd}=0.5$ eV (lowest) to $t_{pd}=2$ eV in steps of 0.5 eV.

effect on the LESW due to the *effective* MH model comparable to the DLESW as found in the preceding section. However, because the t_{pd}-dependent prefactor c already contains some kinetic effect it is not that straightforward to define a DLESW as in the MH case.

In Fig. 13 the d part (left) and p (right) part of the LESW is shown. It is interesting to see that for a hole-doped CT system the dynamical part of the LESW, due to the hybridization between neighboring oxygen and copper orbitals, is almost entirely due to a spectral weight transfer from the d-like UHB to the ligand band near the Fermi level, while no extra p spectral weight is observed in the UHB. This can be seen from the fact that the p-LESW coincides more or less with the $\Lambda(x_h)=x_h$ curve, corresponding with hole doping the CT system without intersite hybridization. For the electron doped CT system and for low doping concentrations, the situation is reversed. Now the dynamical contribution to the LESW is mostly due to extra p spectral weight while the d-LESW follows the $\Lambda(x_e)=2x_e$ curve, corresponding with electron doping the CT system in the localized limit.

The effect of the cluster size on the LESW is also studied. In Fig. 14 we show the LESW for three-, four-, and five-unit-cell CT clusters with $U_{dd}=8$, $t_{pp}=-0.25$, $\Delta=4$, and $t_{pd}=1$ eV. From the figure it can be seen that, as in the MH case, the size of the cluster is of little or no importance to the LESW.

IV. DISCUSSION AND CONCLUSIONS

For the Mott-Hubbard (MH) system, in which the low-energy spectral weight (LESW) is symmetric with respect to hole or electron doping, we found that the LESW grows faster than two times the amount of doping when the hybridization is taken into account. The LESW may be divided into two parts, the static LESW (which is just the result of counting the available states) and a dynamical part (DLESW), which is the kinetic contribution. The DLESW is strongly dependent on the intersite hybridization and on the amount of doping but independent on cluster size and dimensionality. We could identify a sort of critical doping concentration for which the DLESW reaches its maximum. This critical concentration also seems to be related to the turn over from electron to hole-like behavior. This turn over was studied by looking at the lattice parameter dependence of the electron density. For a nearly empty band in a MH model, electrons move towards regions with smaller lattice parameters and larger bandwidths, whereas at an electron concentration above the critical concentration of roughly 0.6–0.7 (doping concentration 0.4–0.3) the electrons move towards the lower bandwidth regions. For large doping concentrations the situation is similar to that of an independent particle picture where electrons like to be in that part where they gain the most kinetic energy.

The CT system shows asymmetric behavior between electron and hole doping when the intersite copper-oxygen hybridization is small. Holes residing on oxygen now occupy almost free-particle levels and scatter weakly off the copper spins. In this region it is therefore not possible to reduce the problem to a (strongly correlated) single-band Hubbard or t-J model. However, when the

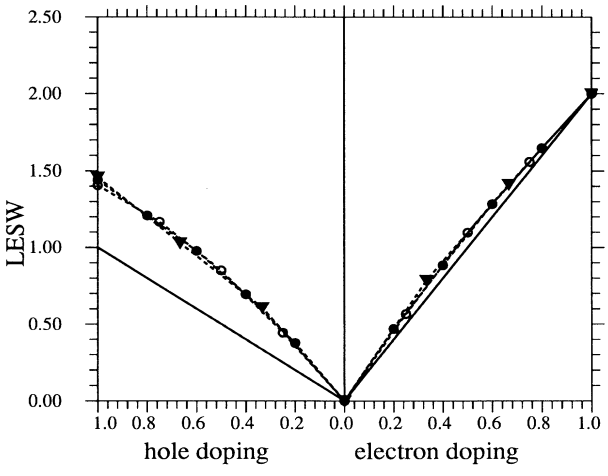

FIG. 14. The LESW as a function of the doping concentration for the CT model for the one-dimensional five-unit-cell (●), five-unit-cell (○) and three-unit-cell (▽) clusters with $U_{dd}=8$, $t_{pp}=0.25$, $\Delta=4$, and $t_{pd}=1$ eV.

hybridization is large, as is the case in the high T_c's the LESW becomes similar to that of the MH system and the electrons as well as the holes show correlated behavior. In this case Cu and O degrees of freedom can no longer be separated in zeroth order. Furthermore, it is shown that the LESW is independent of the cluster size, as for the MH systems, and that the hybridization dependent enhancement of the LESW for hole doping is almost entirely due to the Cu d spectral weight, while for small electron doping concentrations it is almost entirely due to the O p spectral weight.

In mean-field theories, where one describes the eigenstates by a single Slater determinant, the LESW will always be linear with respect to the doping concentration, because the oscillator strength will just be 1 or 0, since spectral weight is now identical to counting states. Unrestricted Hartree-Fock can reproduce the $U \rightarrow \infty$ behavior of the MH model if the holes localize. Linear behavior of the LESW with respect to doping is also found for the t-J model, which behaves the same as the Hubbard model in the localized limit for all values of t and J. The Hubbard I decoupling approximation gives oscillator strengths, which need not be 1 or 0. However, the DLESW calculated in this approximation yields a negative contribution to the total LESW instead of a positive one. The Harris and Lange first order in t/U theory shows that for small t/U the DLESW is proportional to the kinetic-energy expectation value. However, for larger t/U values and for low doping concentrations the first-order expression highly underestimates the DLESW.

The strong dependency of the LESW on the hybridization and doping concentration has interesting consequences for the model Hamiltonians used to describe the low-energy physics. This is because of the fact that the number of effective particles in the low-energy regime is a function of the hybridization and therefore of the volume, temperature and electron-phonon interaction. Therefore, it may well be impossible to define a low-energy-scale Hamiltonian, which describes temperature and pressure dependent properties unless one introduces a kind of effective nonparticle conservation and fractional statistics.

ACKNOWLEDGMENTS

We would like to acknowledge useful discussions with D. I. Khomskii, M. J. Rice, A. M. Oleś, and L. F. Feiner. This investigation was supported by the Netherlands Foundation for Chemical Research (SON) and the Netherlands Foundation for Fundamental Research on Matter (FOM) with financial support from the Netherlands Organization for the Advancement of Pure Research (NWO).

[1]E. H. Lieb and F. Y. Wu, Phys. Rev. Lett. **20**, 1445 (1968).
[2]P. W. Anderson and Y. Ren, *Proceedings of the Los Alamos Symposium on High Temperature Superconductivity,* edited by K. S. Bedell *et al.* (Addison-Wesley, Reading, MA, 1989).
[3]H. J. Schultz, Phys. Rev. Lett. **64**, 2831 (1990).
[4]J. B. Grant and A. K. McMahan, Phys. Rev. B **46**, 8440 (1992).
[5]J. Lorenzana, Ph.D. thesis, International School for Advanced Studies, Trieste, 1992.
[6]V. J. Emery, Phys. Rev. Lett. **58**, 2794 (1987).
[7]K. A. Chao, J. Spatek, and A. M. Oleś, J. Phys. C **10**, 2271 (1977).
[8]C. Castellani *et al.*, Phys. Rev. Lett. **69**, 2009 (1992).
[9]F. D. M. Haldane, Phys. Rev. Lett. **67**, 937 (1991).
[10]C. T. Chen *et al.*, Phys. Rev. Lett. **66**, 104 (1991).
[11]H. Romberg *et al.*, Phys. Rev. B **42**, 8768 (1990).
[12]P. Kuiper *et al.*, Phys. Rev. Lett. **62**, 221 (1989).
[13]S. L. Cooper *et al.*, Phys. Rev. B **41**, 11 605 (1990).
[14]H. Eskes, M. B. J. Meinders, and G. A. Sawatzky, Phys. Rev. Lett. **67**, 1035 (1991).
[15]M. S. Hybertsen, E. B. Stechel, W. M. C. Foulkes, and M. Schlüter, Phys. Rev. B **45**, 10 032 (1992).
[16]Y. Ohta *et al.*, Phys. Rev. B **46**, 14 022 (1992).
[17]P. Unger and P. Fulde (unpublished).
[18]J. Hubbard, Proc. R. Soc. London, Ser. A **276**, 238 (1968).
[19]J. Zaanen, G. A. Sawatzky, and J. W. Allen, Phys. Rev. Lett. **55**, 418 (1985).
[20]E. Dagotto *et al.*, Phys. Rev. B **41**, 9049 (1990).
[21]I. Sega and P. Prelovšek, Phys. Rev. B **42**, 892 (1990).
[22]H. Matsumoto, M. Sasaki, and M. Tachiki, Solid State Commun. **71**, 829 (1989).
[23]M. A. van Veenendaal, R. Schlatmann, G. A. Sawatzky, and W. A. Groen, Phys. Rev. B **47**, 446 (1993).
[24]J. W. Allen *et al.*, Phys. Rev. Lett. **64**, 595 (1990).
[25]See, e.g., O. Gunnarsson and K. Schönhammer, Phys. Rev. B **28**, 4315 (1983).
[26]A. B. Harris and R. V. Lange, Phys. Rev. **157**, 259 (1967).
[27]A. Moreo and E. Dagotto, Phys. Rev. B **42**, 4786 (1990).
[28]H. J. Schmidt and Y. Kuramoto, Phys. Rev. B **42**, 2562 (1990).
[29]E. R. Gagliano, C. A. Balseiro, and M. Avignon, Europhys. Lett. **12**, 259 (1990).
[30]F. C. Zhang and T. M. Rice, Phys. Rev. B **37**, 3759 (1988).
[31]L. F. Feiner (unpublished).